Development and Application of a Physics-Based Computational Tool to Simulate Helicopter Brownout

Andrea D'Andrea

Rotor Aerodynamics Technical Leader
AgustaWestland, Aerodynamics Dept.
Lysander Road, Yeovil, UK (BA20 2YB)
andrea.dandrea@agustawestland.com

ABSTRACT

Helicopter brownout has led to numerous accidents in particular during the last military operations in the Gulf theatre. For this reason, the accurate prediction of such phenomenon is currently challenging the global helicopter aeromechanics community in several ways. In this paper, the ongoing development in AgustaWestland of an advanced physics-based numerical tool able to analyze rotorcraft operations in brownout conditions is presented together with several examples of its application. By means of such computational chain, AgustaWestland is investigating enhanced rotorcraft aerodynamic solutions that may be retrofitted to present aircrafts and incorporated in future designs in order to seriously mitigate brownout. With the aim to contribute to a further extension on brownout knowledge, different rotorcraft configurations are analyzed in the course of this work taking into account different flight conditions in ground effect. More in detail, the capabilities of a single-rotor configuration (which characteristics are based on Puma HC1 helicopter) to operate in desert environments are compared to those ones exhibited by a dual-rotor system (tiltrotor – based on V22 sizing and geometry). In the final stages of this paper, numerical simulations carried out on the AgustaWestland AW101 helicopter are reported in order to show how present computational tool is able to catch the well-known experimental evidence of the enhanced capabilities of present helicopter to mitigate brownout.

INTRODUCTION

Helicopter taking-off and landing in dry sandy or powdery snow conditions usually experience brownout or whiteout phenomena where the rotor downwash creates a cloud of dust or snow that can dramatically reduce pilot visibility to zero. In case of brownout, dust can cause a total loss of situational awareness because visual references become not visible. This fact can involve possible collisions with unseen obstructions or cause lateral drift during the touchdown generating dramatic rollover motions of the rotorcraft. Helicopter brownout has led to numerous accidents in particular during the last military operations in the Gulf theatre [1]. By a rough estimation, approximately the 75% of whole rotorcraft crashes occurred in Iraq and Afghanistan has been attributed to this phenomenon. Extended operations in brownout conditions are extremely worrying even because the entrainment of sand and debris can bring to serious damages of both engine components and rotor blades, or to a lost of engine power in take-off due to the filters clogging. Helicopter brownout generally occurs dependent on numerous factors. Rotorcraft disk loading and its configuration, soil composition, wind, helicopter landing trajectory, all affect the entrainment and circulation of ground dust, sand and debris during operations in desert environments. Conventional single-rotor helicopters (Figure 1) are severely affected because the unsteady rotorwash creates swirling dust clouds around the fuselage. In dual-rotor systems (tandems and tiltrotors - Figure 2) the situation seems to be even worse, due to the presence of the so-called 'fountain effect' in the middle region within the two rotors.

The accurate prediction of rotorcraft brownout is currently challenging the global helicopter community in different ways. Several works have been carried out in the last years by means of both experimental rotor tests and numerical simulations to further improve the knowledge on this subject. Recent numerical works reported in literature [3]-[5] are presently demonstrating that specific aerodynamic modifications to a rotorcraft may offer several advantages in terms of pilot visibility. In effect, experimental evidence coming from the Gulf theatre is confirming improved brownout characteristics of some helicopters over other ones. The AgustaWestland AW101 (Figure 3), for instance, has been flown by the RAF 28° Sqn. in Jordan, Kenya and Iraq in unbelievable dry dusty-sandy environments. In such cases more than 12,500 landings were led without incidents caused by brownout [2]. It is by now very well recognized that present helicopter is able to generate a region of clear visibility around the fuselage that allows both safety operations in sandy-desert environments, and avoids running landings and takeoffs of the helicopter (usually recommended in dusty conditions) which can result in many broken landing gears or more serious accidents. The evidence of the great capability of AW101 to avoid brownout, is just a demonstration of the possibility to generate advanced helicopter designs able at least to mitigate such phenomenon. On this basis, rotorcraft manufacturer companies are currently strongly busy to investigate aerodynamic solutions that can be retrofitted to present rotorcrafts and incorporated in future designs, nevertheless without degrading the overall performance of the aircraft.

Additional recent works, which have tried to enlarge general comprehension of brownout phenomenon, are for instance those ones reported in Ref. [4] and [6] by Phillips and Brown, where the effects on the onset and development of brownout (in terms of both extension and compactness of dust clouds) produced by different helicopter configurations were analyzed. In these works, the authors introduced an innovative *Eulerian*-computational model based on an approximation of the full-dynamics of the coupled particulate-air system. Present model was based on the assumption that suspended particulate matter may remain in near equilibrium under the action of the aerodynamic forces

as soon as they fluctuate in the free air far away from the soil. Close to the ground, on the contrary, the previous hypothesis was replaced by a sublayer type source-model in which the saltation process was modeled algebraically. In these works, the unsteady aerodynamic environment was modeled by means of Brown's Vorticity Transport Model [7] (VTM) fully reported in literature. Numerical results reported in [4] clearly highlighted the better capability of a conventional single rotor aircraft to operate in brownout conditions with respect to tandem configurations.

Figure 1. HH-60G Pave Hawk helicopter operating in brownout conditions

Figure 2. V22 tiltrotor operating in sandy-desert environments

In the same way D'Andrea ([3] and [8]) further extended previous works by using an innovative potential numerical tool coupled with a *Lagrangian*-computational model for particles transportation, comparing single- rotor, tandem and tiltrotors. Numerical results reported in these works showed that both shape extension and compactness of sand-clouds are directly related to a change in mode within the flowfield surrounding the various rotorcrafts in the different flight regimes occurring when operating IGE. In case in fact of a single-rotor-configuration, flight operations within 'recirculation regimes' were found to generate the greatest entrainment of dust and sand, since the ground particles tend to follow the air streamlines and the vortex structures that recirculates through the forward part of the rotor disk. High levels in velocity-unsteadiness were found to occur in the zone immediately forward the fuselage just before the entry in 'ground-vortex regimes'[3]. In case of a tandem or a tiltrotor, the aerodynamic environments around the aircrafts were found to be much more worrying in terms of a brownout perspective. Tandem, for instance, was showed to produce (for equivalent values of aircraft speeds) larger and stronger ground vortex structures in recirculation regimes, while tiltrotors were shown to generate wide zones of unsteady upwash and recirculation in the region within the two rotors which both concurred to a huge amount of sand particles lifted from the ground and surrounding the fuselage.

Figure 3: AgustaWestland-AW101 enhanced capability to mitigate brownout

Main goal of this work is to introduce and present the ongoing development in AgustaWestland of an advanced physics-based numerical tool able to analyze rotorcraft operations (even in unsteady maneuver, when coupled with Flight Mechanics code) in brownout conditions, producing unique results in numerically predicting both the aerodynamic field generated by a rotorcraft operating on ground, and at the same time to determine the consequent shape extension and compactness of the dust cloud surrounding the helicopter in brownout operations. By means of such computational chain, AgustaWestland is presently investigating enhanced rotorcraft aerodynamic solutions that may be retrofitted to present aircrafts and incorporated in future designs in order to seriously mitigate brownout. Present numerical computational chain will be presented together with different examples of its application. More in detail, the capabilities of a single-rotor configuration (which characteristics are based on Puma HC1 helicopter [9]) to operate in desert environments are compared to those ones exhibited by a dual-rotor system (tiltrotor – based on V22 sizing and geometry [10]). Aim of such analyses will be numerically demonstrate the 'anecdotal evidence' of the better capabilities of single-rotor helicopters to operate in sandy-desert environments with respect to tiltrotors. In the final stages of this paper, numerical simulations carried out on the AgustaWestland AW101 helicopter are reported in order to show how present computational tool is able to catch the well-known experimental evidence of the enhanced capabilities of present helicopter to mitigate brownout.

NUMERICAL METHOD

The AgustaWestland 'Brownout-Simulation Tool', which was originally presented in part in Ref. [14], is composed by four different elements, that are: FLIGHTLAB, TOP (Trajectory Optimization Program), ADPANEL-RAS (Rotorcraft Aerodynamics Solver) and ADPANEL-PTM (Particle Transport Model), which are visible in the flowchart depicted in next Figure 4.

The flight mechanics helicopter maneuver, that has to be simulated in brownout condition, is at first analytically estimated using the commercial software FLIGHTLAB [11], through a 'Trajectory Optimization Approach' which allows evaluating the control time histories and the ensuing vehicle response by minimizing a suitable cost function while satisfying specific trajectory constraints. Typically a maneuver can be evaluated through a forward integration of the model dynamic equations, for given control time histories and a specific vehicle initial condition. With this approach, generally, the analyst has to perform several trials in order to

satisfy specific trajectory requirements defined during the maneuver and/or related to the final vehicle configuration. On the other hand, the main advantages of the trajectory optimization approach with respect to the classical 'trial and error' forward simulation is based on the fact that the maneuver requirements are systematically fulfilled through constraints of the optimization problem, and the resulting maneuver is in some sense optimal according to the specification of the cost function. To this purpose, the Trajectory Optimization Program TOP [12] has been coupled to the commercial software FLIGHTLAB. The flight mechanics model used for the simulations is based on three-dimensional rigid body dynamics, where rotor forces and moments are computed by using an actuator disk model with uniform inflow. Look-up tables are used for the quasi-steady aerodynamic coefficients of the vehicle lifting surfaces.

Once that the helicopter landing maneuver has been assessed by means of the previous optimization process (FLIGHTLAB-TOP), a more advanced aerodynamic tool is used to determine the complex unsteady aerodynamic flowfield close to the ground (necessary to accurate simulate IGE states). To this purpose, previous landing trajectories are numerically simulated with the code ADPANEL-RAS [13] (Rotorcraft Aerodynamic Solver), described hereinafter in the course of this work. The entrainment of sand particles and ground debris in the free air surrounding the aircraft is finally computed by means of the code ADPANEL-PTM [3] (Particle Transport Model) once that the unsteady aerodynamic environment has been calculated during the entire landing maneuver.

Aim of the next sections is to further describe in detail previous numerical tools.

Maneuver Design as an Optimal Control Problem

A maneuver can be defined as a finite-time transition between two trim conditions [19]. Clearly, given a starting condition and an arrival condition there is an infinite number of ways to transition between the two. A way to remove this arbitrariness is to formulate a maneuver as an 'optimal control problem' [20], where one minimizes a cost (time, altitude loss, control activity, fuel consumption, etc.). The term trajectory optimization refers to the process of computing the optimal control inputs and the resulting response of a model of a vehicle, a rotorcraft in the present case, that minimize a cost function (or maximize an index of performance) while satisfying given constraints (which specify, for example, the vehicle flight envelope boundaries, and/or safety and procedural requirements for a maneuver of interest). Notice that this problem differs significantly from the usual and more common problem of forward simulation starting from given initial conditions under the action of control inputs, both in the case when the control time histories are given a priori, or when they are computed by a flight control system or tracking controller.

The vehicle mathematical model is typically regulated by a set of Ordinary Differential Equations (ODEs) which can be written as:

$$\dot{f}(x, x, u, t) = 0 \tag{1a}$$

$$y = h(x) \tag{1b}$$

where x is the state vector, while the vector u collets the flight controls. The vehicle model is completed by Eq. (1b), which defines a vector of outputs y. The outputs will typically represent some global vehicle states that describe its gross motion, such as position, orientation, linear and angular velocity of a vehicle-embedded frame with respect to an inertial frame of reference, or other quantities useful for formulating the maneuver optimal control problem.

Equations (1a) are solved for the forward simulation problem by providing a time history of control inputs u(t) and initial conditions on the states $x(0) = x_0$. Accordingly, one obtains also the associated values of the outputs through (1b). The trajectory optimization problem is defined on the interval $\Omega = [0;T]$, where the final time T is typically unknown and must be determined as part of the solution to the problem. The Maneuver Optimal Control Problem (MOCP) consists in finding the control function u(t) (and hence through (1) the associated function x(t) and y(t)), and possibly the duration T that minimize a cost function, i.e.

$$\min_{x,y,u,T} \; J(y,u,T) \tag{2a}$$

$$s.t.: \quad \dot{f}(x, x, u, t) = 0 \tag{2b}$$

$$y = h(x) \tag{2c}$$

$$g(x, y, u, t, T) \le 0 \tag{2d}$$

The optimization is subjected to a number of conditions. These include the vehicle equations of motion (1), now appended as equality constraints (2b) in problem (2), together with boundary (initial and/or terminal) conditions on the states, as well as all other maneuver-defining and/or envelope-protection constraints, which have been grouped together and expressed as generic algebraic non-linear constraints in Eq. (2d).

In literature two families of methods are used to solve numerically the Maneuver Optimal Control Problem (2), i.e. the direct and indirect methods. Our Trajectory Optimization Program (TOP), developed at the Politecnico di Milano, is based on direct approaches which are convenient for a series of practical advantages with respect to the indirect ones, and implements multiple evaluation strategies. Details of the methodologies used in TOP can be found in Ref. [12].

Flight Dynamics Maneuver Evaluation

The flight dynamics model used in the numerical applications is a FLIGHTLAB [11] model representing the aircraft. It is based on three-dimensional rigid body dynamics, where rotor forces and moments are computed by using an actuator disk model with uniform inflow. Look-up tables are used for the quasi-steady aerodynamic coefficients of the vehicle lifting surfaces. The vehicle controls are defined as $u = (\theta_{MR}; \theta_{TR}; A_1; B_1)^T$, where θ_{MR} is the main rotor collective, θ_{TR} is the tail rotor collective, A_1, B_1 are the lateral and longitudinal cyclics, respectively. A simplified ground effect model is included in order to properly simulate IGE operations. The objective function used for the optimal trajectory evaluation is the following:

$$J = T + \frac{1}{T}\int_0^T \dot{u} \cdot W \, \dot{u} \, dt \tag{3}$$

In this expression the first term enforces an aggressiveness parameters, i.e. the maneuver duration, while the second one weights the piloting control effort [12]. The relative importance between these two antithetic terms is regulated by the matrix of weights $\boldsymbol{W}$.

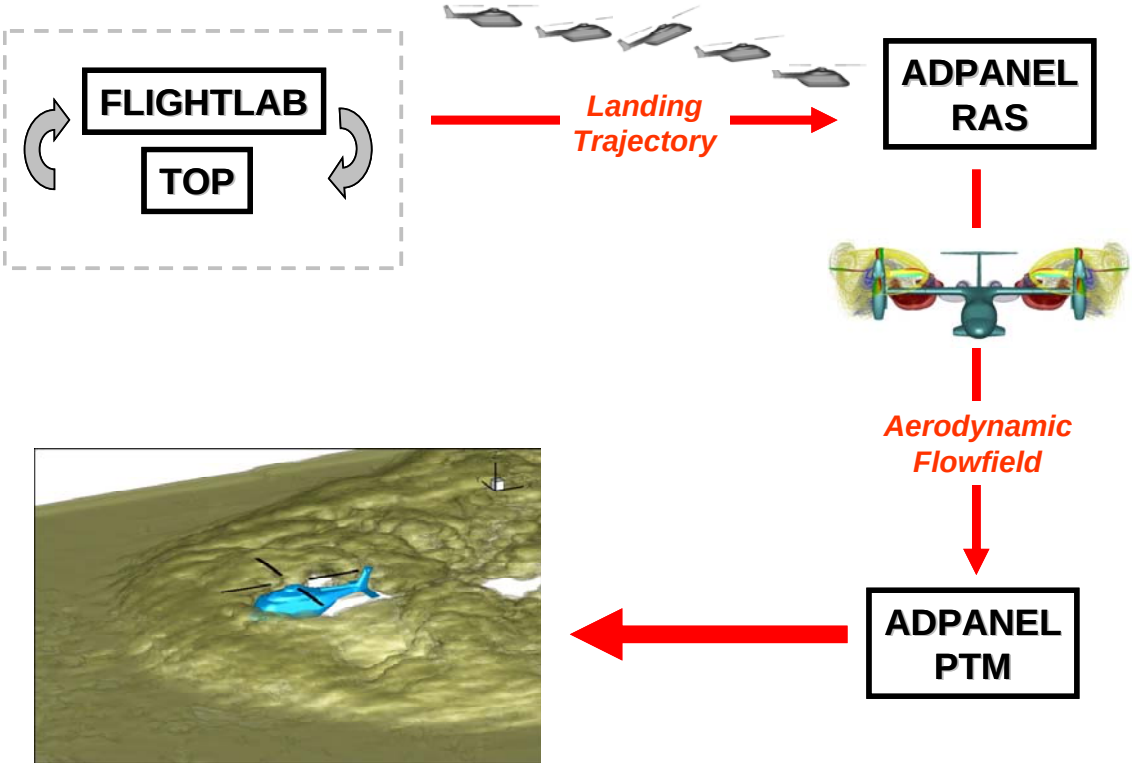

Figure 4: Flowchart of the AgustaWestland 'Brownout Simulation Tool' (FLIGHTLAB, TOP, ADPANEL-RAS and ADPANEL-PTM)

In particular as the norm of this matrix is reduced, the minimum time requirement becomes more important and the maneuver is more aggressive, thus requiring a more intense pilot activity. The weights in ***W*** are chosen in order to obtain a proper compromise between the maneuver duration and control activity.

ADPANEL – Rotorcraft Aerodynamics Solver (RAS)

Main element of the AgustaWestland brownout simulation tool is the code ADPANEL-RAS (Rotorcraft Aerodynamics Solver). This code [13] is a full-unstructured panel method coupled with a time-stepping full-span free wake vortex model. Present tool implements the most advanced aerodynamic features in the field of potential methods, such as the capability to represent the geometrical surfaces into unstructured-hybrid meshes (it can handle with both quadrilateral and triangular cells), for a Constant Vorticity Contour (CVC) modeling of both rotary and fixed wing wakes, and for its Multi-Processor implementation. Thanks to the previous features, ADPANEL is able to analyze in short computational times and with detailed predictions entire helicopters and tiltrotors configurations even operating in ground effect.

The wake modeling implemented in ADPANEL is composed of two parts: a 'dipole buffer wake sheet', and a set of 'Constant Vorticity Contour vortex filaments'. Buffer wake and CVC vortex filaments are used to represents the vorticity released from rotary and fixed wings for both their components, trailed and shed. The Constant Vorticity Contour free-wake modeling developed in ADPANEL allows to generate refined roll-ups and high spanwise resolution along rotor blades without enforcing an unnecessary large number of wake elements. Figure 5 shows an example of the computed CVC wake development in case of a tiltrotor operating out of ground effect. Recent and validated 'vortex dissipation laws' [15] have been implemented in ADPANEL in order to represent the increasing of the vortex core with the time passing, as well as 'vortex-straining-models' such as those ones developed by Bhagwat and Leishman [16], both fundamental in case of IGE helicopter simulations. Detailed additional information regarding both theory and validation of present numerical tool can be found in Ref. [13].

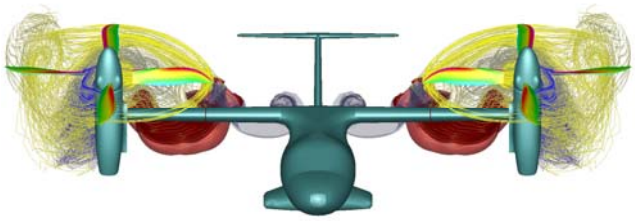

Figure 5. ADPANEL CVC wake development of the ERICA Innovative Tiltrotor in descent flight condition

ADPANEL – Particle Transport Model (PTM)

A Particle Transport Model (PTM) has been implemented in ADPANEL by using a Lagrangian approach. In this model, the entrainment of dust and ground debris in the free air around the aircraft is realized tracking a very large number of individual particles (even up to five millions) in a direct way using simple equations such as Stokes-type drag laws coupled with inertia. Generally, computational tools based on a Lagrangian approach are normally subject to strong requirements in terms of both computational times and RAM computer memory. This problem was solved in ADPANEL-PTM solver by using a multi-processor (MPI) implementation.

In the Lagrangian frame of reference the dynamics of a single particle is given by Newton's second law:

$$m_p \frac{dv_p}{dt} = F \qquad (4)$$

With the realistic hypothesis that gravity and aerodynamic forces (drag) are the dominant ways for particles motion in free air, a Rayleigh's expression can be used to track their paths. Hence, the first equation is normally coupled with the following:

$$F(u) = -\frac{1}{2}\rho|u|u\frac{\pi d_p^{\,2}}{4}C_d + m_p g \qquad (5)$$

where u represents the particle velocity relative to the air, m_p and d_p, respectively, the particle mass and diameter, and Cd its drag coefficient (in all computations presented in this paper we used the formula Cd = 24/Re).

It can be stated that equation (5) is fully valid only when a particle is free to move in the air and does not lie on the ground. In effect, in this case, the physics of the occurring phenomena is much more complicated. If from one side we could maintain that in order to be moved by rotorcraft flowfield a sand particle must assume a minimum horizontal velocity able to overcome the sliding friction acting on it, from the other, we have to state that real situation for particle pick-up from ground is highly more complicated. Marticorena and Bergametti [17] asserted that the entrainment of sand and dust particles in the free air can occur only whether the velocity above the ground surface overcome a minimum (or 'threshold') value. In this case, the largest particles start to move hopping on the other ones (process of 'saltation'), causing further ones to be ejected away from the soil. Particle with less inertia (such as the smallest) do not come back on the ground, but are entrained into the flow. Bagnold [18] proposed a compact simple formula for evaluating the threshold velocity based on the main characteristics of sand particles (density and diameter). The final formulation proposed by Bagnold, can be summarized in the following:

$$v_t = A\sqrt{\frac{\rho_p - \rho}{\rho} + \frac{\beta}{d_p \rho}} \qquad (6)$$

where A = 0.1109 and β = 3×10-4 Nm-1.

In the ADPANEL Particle Transport Model (PTM) the previous equation (5) is numerically computed by using the unsteady solution provided by the Rotorcraft Aerodynamic Solver (RAS). Equations (4) is subsequently integrated in time by using a second-order accurate scheme. Following the previous statements, before starting the numerical computation, the PTM model evaluates the threshold velocities corresponding to the salting particle diameters. With the aim to represent as much as possible the chaotic characteristic typical of brownout conditions, several values of sand particles diameters are generally modeled in ADPANEL. Generally, the computations are carried out by using values of sand particles diameters all in the range [2μm-50μm] with a unique value of sand density (2650 kg/m^3). The overall number of particles tracked by this code is never less than one million, and in case of the finest simulations can arrive up to 5 millions.

The aerodynamic solution for helicopter applications in ground effect is normally evaluated every 5° of main rotor blade azimuth, in order to guarantee realistic wake structure deformations and vortex roll-ups when impinging on ground. Depending on user's input settings, every *n-steps* the Rotor Aerodynamics Solver computes the induced velocities generated by all rotors, airframe and wakes (together with the effect of the ground) in a predefined computational volume widely enclosing the aircraft (called 'scan-volume'). Brownout simulations will be consequently possible only in that region. At the end of the RAS computations, the induced velocities are known in the entire volume for several different time steps. During the Lagrangian particle tracking, the total velocity corresponding to a generic position of a sand particle is assessed interpolating by means of 'inverse distance formula' the velocity values at the eight scan-volume cells' vertices. Since the tracking of particles normally requires very small computational time steps, scan-volume solutions are furthermore interpolated in-time in a linear way. Since both Navier-Stokes (RANS) and potential methods are able to provide only time-averaged aerodynamic solutions, stochastic models of unsteady turbulent fluctuations are implemented in ADPANEL-PTM with the aim to further improve computations to represent the chaotic characteristics typical of real brownout conditions. Additional detailed information regarding both theory and implementation of present numerical tool can be found in Ref. [3].

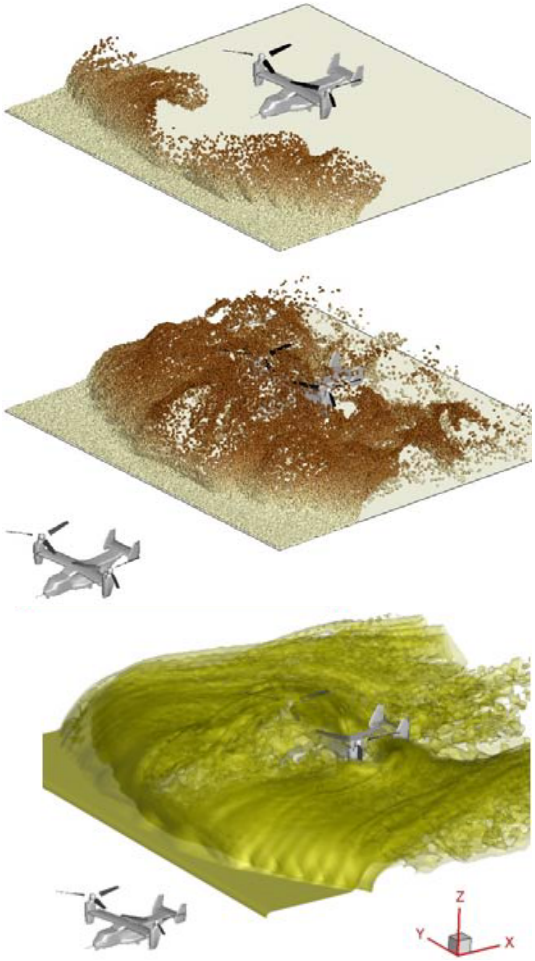

Figure 6. Example of numerical results provided by the ADPANEL-PTM solver

Multiple-picture reported in Figure 6 gives an example of typical numerical results provided by the ADPANEL-PTM model. It can be clearly seen (top row) the insertion of the sand particles in the computational volume (that is moving together with the aircraft) at the beginning of the computation, as well as the starting of the generation of the dust cloud surrounding the helicopter (middle raw). At the end of all PTM computations, particles accumulations in the free space are 'transformed' in particulate-density-levels assessing the quantity of sand mass in every cell of a 'highly-fine volume'. By means of a visualization program, said

density levels are finally plotted with different values of 'translucency' (directly proportional to the inverse of sand density) in order to render believable the brownout scenario around the helicopter (bottom raw - Figure 6).

NUMERICAL RESULTS: PUMA VS. V22

Aim of this section is starting to introduce numerical results with the aim to both highlight the capabilities of the tool, and to increase at the same time the general knowledge on helicopter brownout. To do that, two different rotorcrafts are analyzed and compared between them: a single-rotor helicopter and a tiltrotor. It's worth specifying that although the computational chain is totally able to analyze *unsteady maneuvers* close to the ground (thanks to the coupling with the FLIGHTLAB-TOP tools), in this paper we just focused on steady hover and forward flight conditions. Moreover, every computation reported in this work was carried out without the presence of the fuselage that is often reported only for illustrative purposes.

The single-rotor helicopter analyzed in this section is the Puma HC1. Present helicopter, in force to the Royal Air Force (RAF) which is at present fully operative in theatre [2], is equipped with 4 rectangular-shaped blades. The blades employ a NACA0012 airfoil to achieve a total twist of -8 degrees. Rotor radius is equal to 7.54 m (24.75 ft) and the nominal tip speed is 209.34 m/s. Aircraft weight is fixed in this section at 6,500 kg. Since the not availability of the real CAD model of its main rotor blade from now on we will refer to this rotorcraft as 'Puma-like' helicopter. The geometrical model used in all computations for previous rotorcraft is reported in next Figure 7. Helicopter data were taken from Ref. [9] and are reported for the sake of clearness in next Table 1.

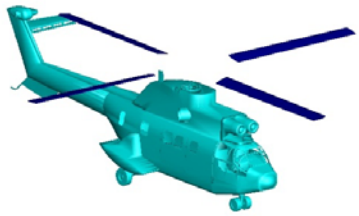

Figure 7. Geometrical model of Puma-like HC1 helicopter

Puma HC1 – from Ref. [9]	
N rotors	1
N blades	4
R (m)	7.54
Vtip (m/s)	209.34
T (N)	63,765
CT (*)	0.0067

(*) *ISA Sea-Level Conditions*

Table 1. Geometrical data of Puma-like HC1 helicopter

The multiple-rotor configuration analyzed in this section is the V22. The geometrical model used in all computations for previous configuration is reported in next Figure 8. As in the case of the Puma, due to the not availability of the real CAD model of its rotors' blades, we will refer to present rotorcraft as 'V22-like' tiltrotor. Geometrical data used in present work were taken from Ref. [10] and are reported in next Table 2. In this case, the aerodynamic sections of the two counter-rotating rotors start with a 36-in chord at 5% radius, linearly tapering to a 22-in chord at the blade tip. The total effective blade twist is enforced to be 47.5° over a 228.5-in radius. Aircraft weight is in this case fixed at 24,000 kg which obviously must be shared between the two rotors.

All the aerodynamic computations carried out by means of the ADPANEL-RAS solver were carried out using a very-fine time discretization (i.e. 5° of main rotor blade azimuth) in order to guarantee realistic wake structure deformations and vortex roll-ups when impinging on ground. The whole numerical calculations were led up to one-hundred (at least) rotor revolutions in order to get accurate predictions of both radial (outwash) and swirl velocities in proximity of the ground.

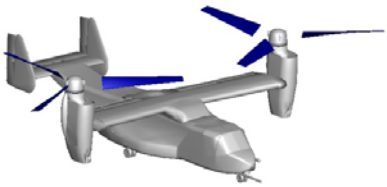

Figure 8. Geometrical model of V22-like tiltrotor

V22 – from Ref. [10]	
N rotors	2
N blades (for each rotor)	3
R1 = R2 (m)	5.80
Vtip1 = Vtip2 (m/s)	201.75
T1 = T2 (N)	117,720
CT1 = CT2 (*)	0.0223

(*) *ISA Sea-Level Conditions*

Table 2. Geometrical data of V22-like tiltrotor

With the aim to highlight the exhibited behavior of previous rotorcrafts while operating in desert environments, different steady-flight conditions were analyzed and main results reported hereinafter in the course of this section. Table 3 summarizes the conditions simulated in this paper; that are: 1a) HIGE at h/R = 3.00; 1b) HIGE at h/R = 1.50; 2) FFIGE at 4.50 m/s (8.75 kts) at h/R = 1.50 (h/R = non-dimensional distance of rotor hub center with respect to the ground).

Condition N.	V (m/s)	V(kts)	h/R
1a	0.00	0.00	3.00
1b	0.00	0.00	1.50
2	4.50	8.75	1.50

ISA Sea-Level Conditions

Table 3. Operative conditions simulated for the Puma-like helicopter and the V22-like tiltrotor

Numerical results in HIGE conditions

Figure 9 depicts the rotor wake structures obtained by means of the ADPANEL-RAS solver for the Puma-like helicopter operating in HIGE at h/R = 3.00 (top) and 1.50 (bottom) respectively. Vorticity magnitude is colored by means of a contour plot. A strong radial stream, is produced in both cases in all the azimuthal directions along the ground plane due to the coupling of the vortex structures with the ground itself. Such radial stream was found to increase in a non-linear fashion with the reduction of the aircraft height (arrowed lines in Figure 9). Pairing and merging phenomena of the blade tip vortices were found to occur very near the ground increasing the unsteadiness of radial and swirl velocities around the helicopter. Additionally, a quite strong

'fountain effect' was found to be present near the blade roots furthermore complicating the overall aerodynamic environment in HIGE conditions around the fuselage, as it can be evident from Figure 9. This fountain effect, was found to increase its magnitude with the reduction of the rotor height.

In case of the V22-like tiltrotor, the effect of the ground were found to be much more pronounced than the one obtained for the previous single-rotor aircraft. The main reasons for this are, without any doubt, the higher disk loading and the production of a 'real-strong fountain effect' directly aroused by the ground. As showed in many other works [21], in fact, there is a strong tendency for a tiltrotor operating IGE to generate highly-unsteady vortical-recirculating zones between the two rotors. This is because the wake of one rotor interacts with the wake of the other, and the global resulting vortex structure is convected in the upward direction due to the presence of the soil. This strong interactional effect is very similar to the 'rotor-on-wing' fountain effect described in literature for tiltrotors. Next Figure 10, on purpose, shows the aerodynamic field on a longitudinal plane passing through aircraft centerline. In present picture, we indicated with a contour plot (red – maximum levels) the vertical induced velocity, and arrows indicate the direction of the global flowfield. Simulations seem to confirm all previous statements highlighting a high-magnitude recirculation zone between the two counter-rotating systems, which produces strong 'positive' vertical velocities all around the aircraft. To further represent the overall flowfield occurring around the V22-like tiltrotor in HIGE, we reported in next Figure 11 a snapshot of the time-development of vorticity field around the aircraft in both analyzed hover conditions. Differently from the Puma-like helicopter, a large amount of unsteady vorticity is produced at both altitudes just below the fuselage and it's convected downstream reaching the ground. Previous conclusions seem to highlight a more worrying situation for the tiltrotor configuration in a brownout prospective. In effect, the V22-like aircraft produces an aerodynamic flowfield that seems to contain much more recirculating zones around the fuselage, with higher values of swirl and positive (upwash) velocities.

Results related to the consequent onset and development of dust clouds generated by previous configurations in hovering are reported in Figure 12 and Figure 13. HIGE results at h/R = 1.50 are reported in the former, which shows different snapshots of the sand-dust clouds time-histories surrounding both the Puma-like (top raw) and the V22-like (bottom) aircrafts. It can be highlighted that at the beginning of the simulations (left column) both aircrafts tend to move out from the computational domain the sand particles due to the presence of a strong radial-stream produced on ground. Very soon, however, the effect of swirl-velocities components (and of the upwash zones) present near the soil start to play a not marginal role allowing many sand particles to be raised from the ground, to be lifted in the free air, and finally to be re-ingested by the rotorwashes. Previous phenomenon of particles re-ingestion is much faster for the tiltrotor configuration, that seems to be almost-totally obscured even in the middle stages of the entire computation (middle column). This result was found to be a direct consequence of the strong upwash generated by present multiple-rotor configuration produced in the spatial zone within the two rotors. It has to be highlighted, as well, the strong non-symmetrical nature of the sand clouds around both configurations (but especially in case of the tiltrotor).

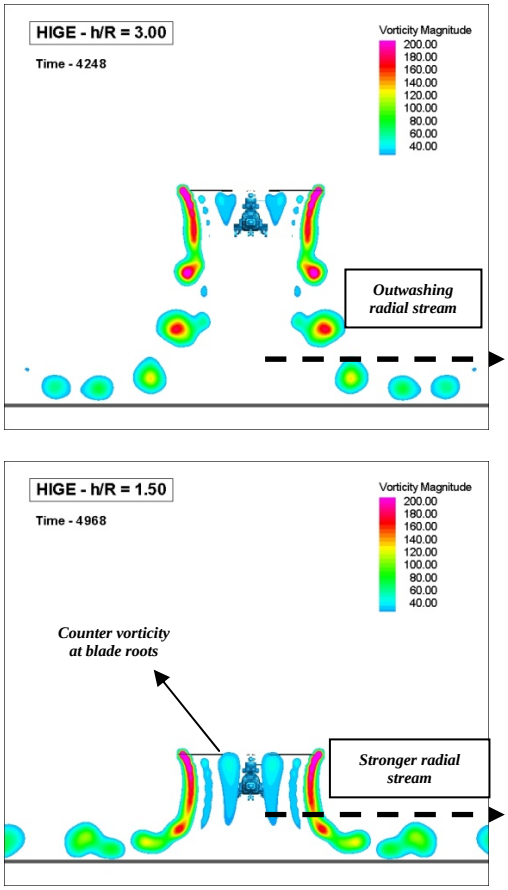

Figure 9. Unsteady development of vorticity field produced by the Puma-like helicopter in HIGE at h/R = 3.0 and h/R = 1.5 [8]

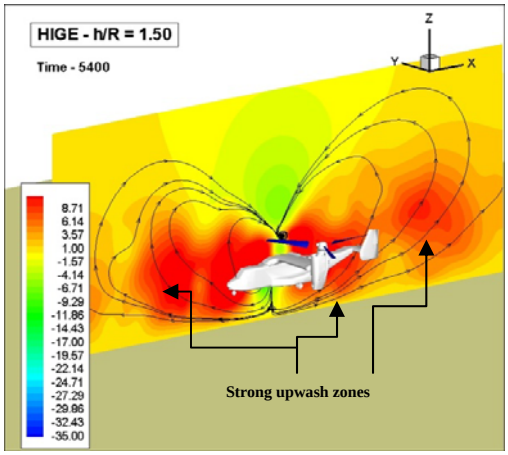

Figure 10. Streamlines and instantaneous induced vertical velocity field for the V22-like tiltrotor, in HIGE at h/R = 1.5 (long. plane through aircraft centerline) [8]

At the end of the entire computations (Figure 12 - right column), i.e. after 10 sec. of operation in brownout conditions, we can state that the V22-like tiltrotor is totally obscured by the cloud dramatically reducing pilot visibility to zero. In the same way, although situation seems to be 'a bit better', swirling dust clouds totally surround the Puma-like helicopter as well, but this just happens at the last stages of the computation. Hence we should highlight, as most important conclusion, that the time needed to completely encapsulate the Puma-like aircraft is much higher than the one needed for the V22-like tiltrotor.

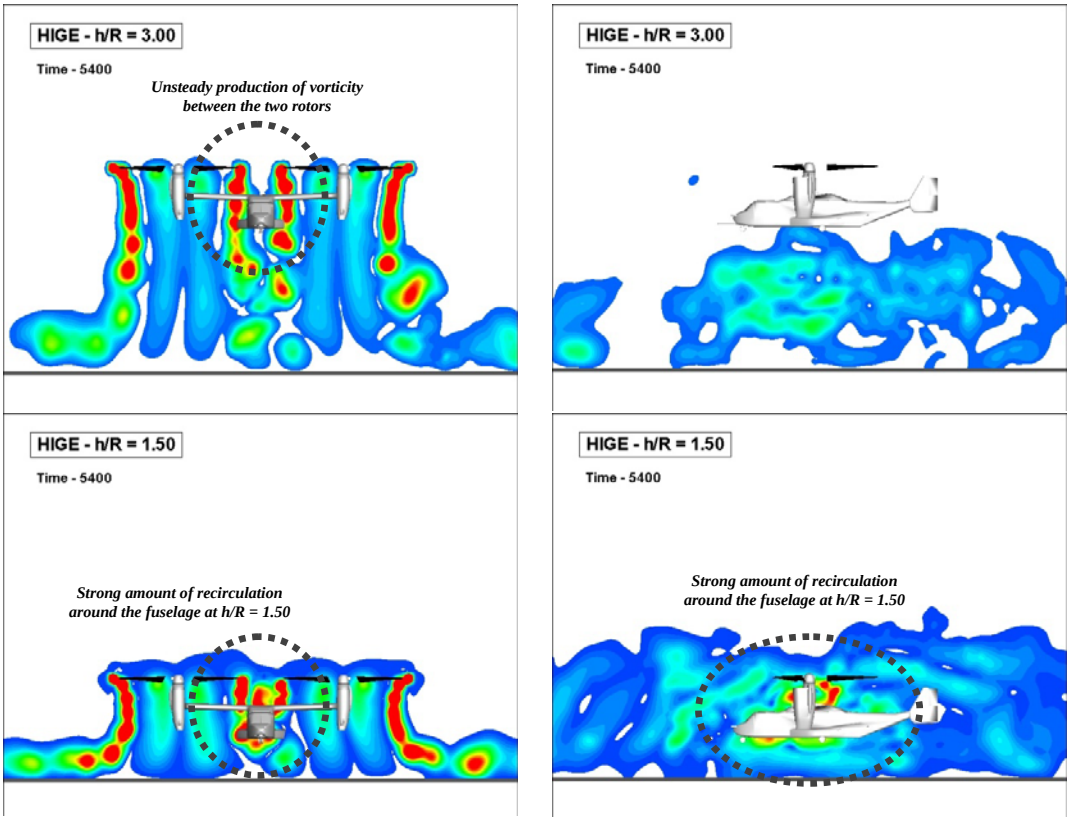

Figure 11. Unsteady development of vorticity fields produced by the V22-like tiltrotor, operating in HIGE at h/R = 3.0 (top) and h/R = 1.50 (bottom) [8]

In Figure 13 we report the comparison in terms of sand cloud geometry and compactness generated around both aircrafts operating in HIGE at the highest altitude (i.e. h/R = 3.00). As previously reported, for higher distance from the ground, the tiltrotor continues to exhibit very large values of vorticity released on ground as well as strong zones of upwash and recirculations just around the fuselage. Hence, if we compare the dust clouds produced by the different rotorcrafts at h/R = 3.00, very-large differences can be found in terms of brownout. In fact (Figure 13 – left side) clearly shows that the Puma-like helicopter seems to be not affected by any re-ingestion of sand particles in the rotorwash, since the strong prevalence of an outwash-radial blowing along the soil with respect to the swirling components. On the contrary, the V22-like tiltrotor clearly shows the same problems already reported for lower altitudes. In effect (Figure 13 – right side), clearly highlights that a huge amount of dust and ground debris are lifted from the ground and recirculated around its fuselage. Hence, results presented up to now, seem to preliminary confirm the anecdotal evidence that single-rotor helicopters have got better behaviors with respect to dual-rotor system configurations [tiltrotor] when operating in brownout in HIGE conditions.

Numerical results in Forward Flight IGE conditions

The forward flight condition analyzed in this work is that one reported in the previous Table 3. Hence, aircrafts altitude is fixed to h/R = 1.50 (altitude of rotor hub center with respect to the ground), and a speed of 4.50 m/s is selected. In present condition, the Puma-like helicopter produces several vortices that form a well defined unsteady-loop recirculating in the forward part of rotor disk. The intermittent nature of velocities close to the ground was found to be caused by a 'separation point – called SP' which displacement is oscillatory in nature. For the normalized advance ratio under analysis, present separation zone occur for the Puma just in front of its fuselage nose, at almost two radius away from the rotor hub. In a brownout perspective, it is believed that large unsteady fluctuations in velocities induced on the ground surface (and, in any case, in proximity of the fuselage) can dramatically increase the entrainment of dust and ground debris in the air surrounding the helicopter, as it will be shown in the next section. Previous unsteady recirculation zone is reported in next Figure 14 (left side). In this picture, the streamlines of the global flowfield are reported in a longitudinal plane through the aircraft centerline coloring them by means of the vorticity magnitude field. Such 'unsteady recirculation zone' just in front of the fuselage nose will be found to be responsible for a large amount of sand particles lifted from the ground and recirculated in the flowfield.

In the same picture (Figure 14 - right side) we report the situation around the V22-like tiltrotor for the same forward flight IGE condition. The first immediate conclusion that can be drawn is referred to the large difference in terms of 'separation point location' with respect to the Puma-like aircraft. In effect, it can be stated that for the tiltrotor the point SP is located at almost six rotor radius far away from the hubs' centers. This fact was found to be due both to the higher disk-loadings of two rotors, but especially to the effect produced by the counter-rotating rotor systems (responsible in HIGE for the production of previous reported huge-upwash through the centerline of the fuselage). Present picture additionally shows as in case of the V22-like the flowfield beyond the separation point is extremely recirculating, as it may be understood by the streamlines paths. As it will be seen hereinafter, present large-recirculation zone will be an important element dramatically affecting the V22-like tiltrotor capabilities to operate in sandy-desert environments.

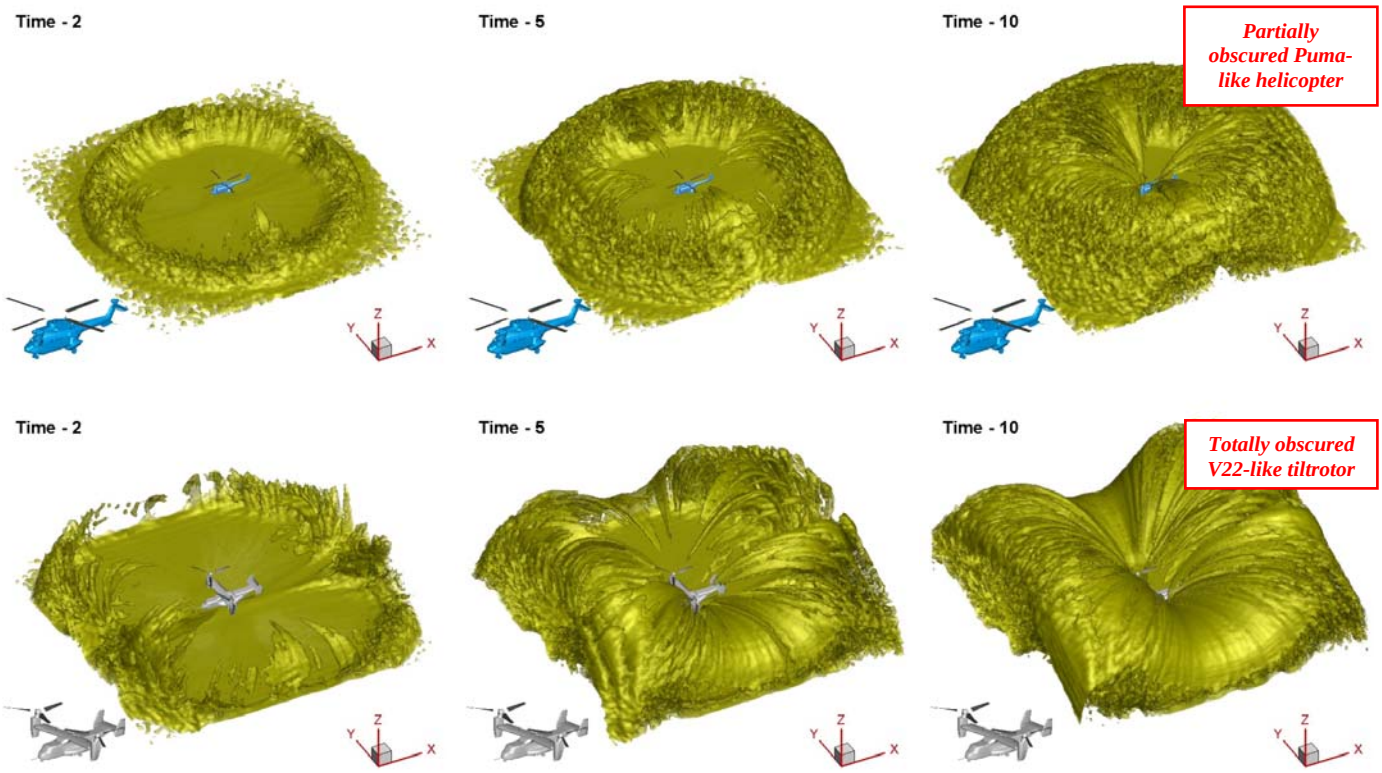

Figure 12. Different snapshots (time-evolution) of the sand-dust cloud generated around the Puma-like helicopter (left side) and the V22-like tiltrotor (right side), operating in HIGE at h/R = 1.5 [8]

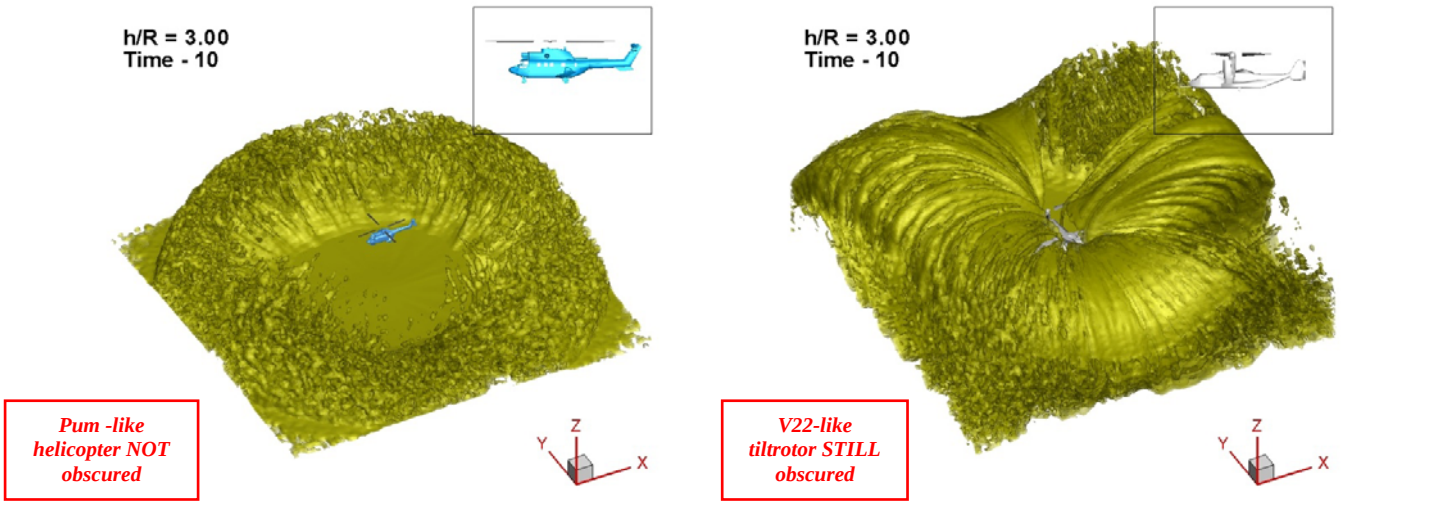

Figure 13. Sand-dust cloud generated around the Puma-like helicopter (left side) and the V22-like tiltrotor (right side), operating in HIGE at h/R = 3.0. Snapshots obtained at the end of the numerical computations [8]

Results discussed up to now, seem to highlight (as in case of operations in HIGE) a much more worrying situation for the tiltrotor configuration in a brownout prospective. To demonstrate that, we made use of the ADPANEL-PTM solver to compute the sandy cloud geometry surrounding the two aircrafts in this specific forward flight condition.

Numerical results are reported in Figure 15, which shows the final sand-dust cloud at the end of the simulations (10 sec of operations). From present picture it can be stated that the behavior of the two different rotorcrafts is very different. In fact, in case of the Puma-like helicopter, a large amount of sand is lifted from the ground at both sides of its fuselage and just in front of the pilot, due the ground-vortex system displaced on the soil that is moving with the helicopter system in the inertial frame of reference. This fact causes an accumulation in time of sand particles just in front of the fuselage nose surely avoiding the pilot to see the ground. We have to state, in any case, that in present situation the fuselage of the Puma-like helicopter is not totally obscured by the dust clouds as it will be showed for the V22-like. In fact, due to the huge values in vorticity released on ground by the tiltrotor (even due to the higher-disks' loadings) the lifted sand-cloud amount seems to be incredibly large even going out (laterally) from the computational domain. Moreover, it can be clearly seen that in case of such dual-rotor system the dust cloud tends to totally encapsulate the aircraft. Once again, as in the case of operations in HIGE, results presented up to here seem to confirm the anecdotal evidence coming from theatre that single-rotor helicopters have got better behaviors with respect to dual-rotor systems [tiltrotors] when operating in brownout conditions.

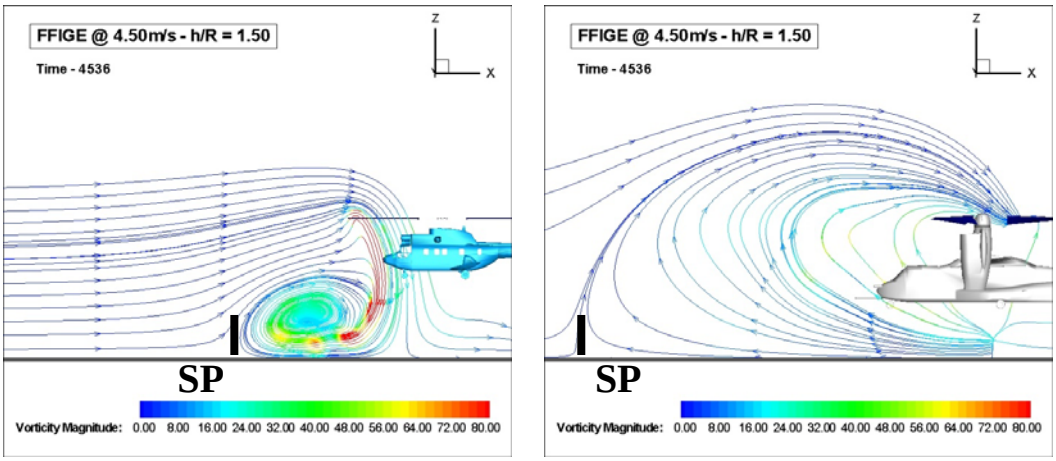

Figure 14. Streamlines of the flowfield [colored with vorticity magnitude] generated in FFIGE conditions (V = 4.50 m/s and h/R = 1.50) around the Puma-like helicopter (left side) and the V22-like tiltrotor (right side) [8]

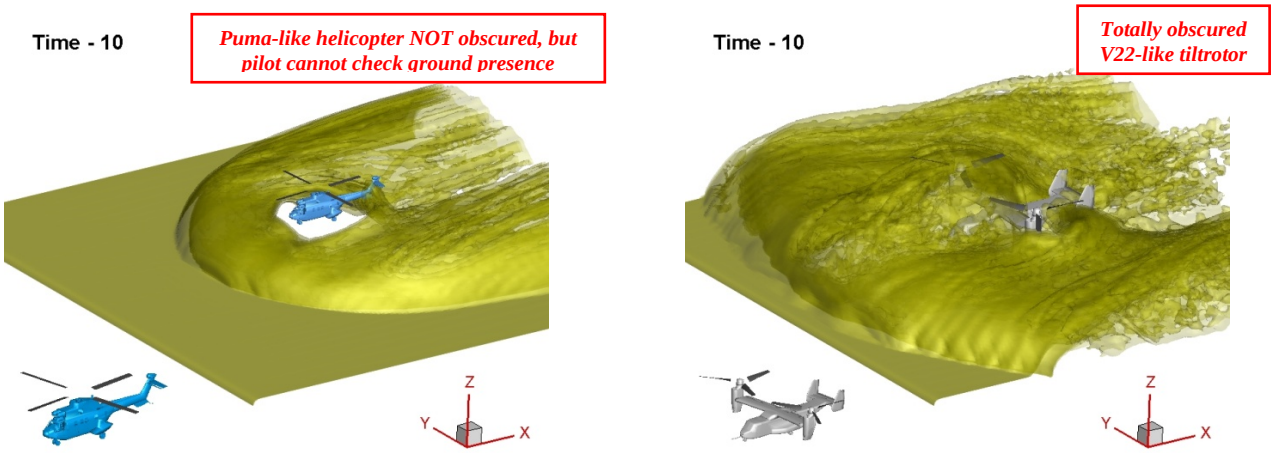

Figure 15. Sand-dust cloud generated around the Puma-like helicopter (left side) and the V22-like tiltrotor (right side), operating in FFIGE conditions at h/R = 1.5 and V = 4.50 m/s

NUMERICAL RESULTS: AW101 VS. PUMA

In this section, the capability of the AgustaWestland AW101 (Figure 16) to operate in desert environment in brownout conditions is analyzed thanks to the presented computational chain, and results are compared with those ones related to the just described Puma-like HC1 helicopter.

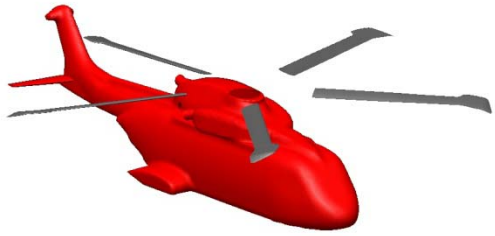

Figure 16. Geometrical model of AW101 helicopter

Geometrical characteristics of the AW101, and the flight conditions that have been simulated and reported in this section, are described hereafter. As for the previous simulations, in present computations no tail rotors have been taken into account as well as the helicopter fuselage which is sometimes reported just for illustrative purposes. The AW101 5-bladed main rotor, equipped with advanced BERP-design blades, is characterized by a rotor radius of 9.2936 m (30.5 ft) with a tip speed is 208.3 m/s. Considering a maximum take-off weight of 15,000 kg, the AW101 operates at a blade loading $Ct/\sigma = 0.101$ if we fix an operation at 1000m and OAT = 40° (as that one analyzed in this section). The Puma-like HC1 was already presented before. The operative blade loading for this aircraft is quite lower than the AW101 one. In fact its Ct/σ is equal to 0.087 since the maximum take-off weight was chosen to be now of 7,000 kg. The landing maneuver considered in this section for the consequent brownout assessment has been simulated considering both rotorcrafts at a constant flight speed of 15 and 10 Kts, in order to represents a possible deceleration before the landing, at one rotor radius distance with respect to the ground (h/R = 1.0).

Aim of this first part is to report numerical results related to the IGE forward-flight operations at 10 Kts. The capability of the AW101 to generate the maximum swirl velocities (vortical structures) quite far from the fuselage nose, is well evident in present forward-flight condition. In effect, next Figure 17 clearly confirm this statement, and moreover it shows that in case of the Puma-like aircraft a 'strong-zone of vorticity' is generated very close to the airframe. Since sand particles that normally compose desert soils in Iraq and Afghanistan are very little (normally, their diameter is assumed to be in the range of 2-10 microns [17]) they tend to strongly follow the air-streamlines. Atmospheric turbulence,

however, may further complicate the situation. Hence, in case of Puma-like operations in low-speed forward flight conditions, it is expected from Figure 17 that a large cloud of dust and ground debris will be formed just in front of the fuselage nose. ADPANEL-PTM numerical simulations totally confirmed such statement. In the following Figure 18, for instance, we report the sand-cloud geometry surrounding both aircrafts. Same levels of sand-density were used to produce this picture. It can be appreciated that the AW101 is able to generate a 'region of clear visibility' in front of the leading edge of the main rotor disk. Next Figure 19 is even more interesting, since it shows the compactness of the consequent sand-clouds generated. In present picture, zone colored in 'brown' represent zones of high-level of sand density (we made use of an exponential-scale to plot the different sand-density levels).

Numerical results related to the forward-flight operations at 15 Kts and h/R = 1.0 are qualitatively very similar to those ones just presented at lower speed. Once again, the AW101 unique capability to generate vortical structures on ground far away from the aircraft will allow to generate less intense and more distributed dust-sand clouds when operating in brownout conditions. For present flight (Figure 20) the Puma-like helicopter in fact tends to generate a vortex-structure that is 'more intense' in magnitude and 'much closer' to the fuselage than the AW101. Hence, even for this operative flight condition, it is expected that Puma-like helicopter can form a larger cloud of dust and ground debris in front of the fuselage nose. ADPANEL-PTM numerical simulations totally confirmed such statement, giving once again a clear indication of which problems can occur in case of operations with Puma-like aircraft in desert environments. In effect, Figure 21 shows that an enormous amount of sand and ground debris is lifted from the desert soil and finally recirculated in the forward part of the rotor disk for the Puma-like. Once again, the sand-cloud seems to be much smoother and further from the airframe nose in case of the AW101 confirming the experimental evidence coming from theatre.

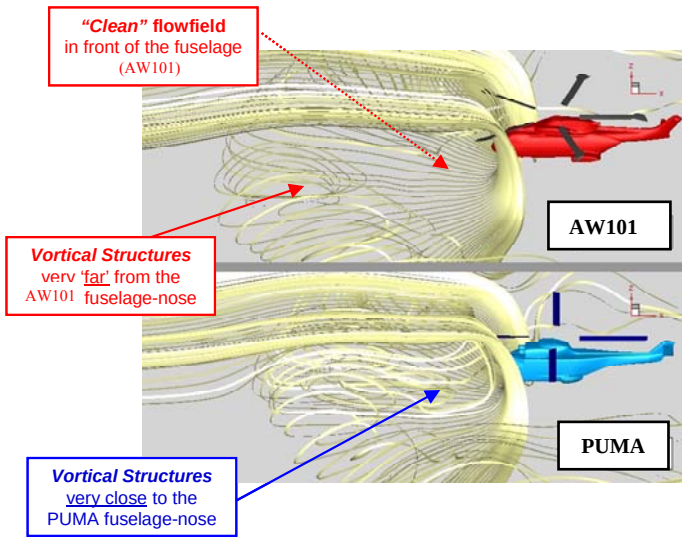

Figure 17 Numerically computed streamlines around the AW101 (top) and the PUMA-like (bottom) for a slow-speed forward flight @ 10 Kts [h/R = 1.0]

CONCLUSIONS

Helicopter brownout has led to numerous accidents in particular during the last military operations in the Gulf theatre. For this reason, the accurate prediction of such phenomenon is currently challenging the global helicopter aeromechanics community in several ways.

In this paper, the ongoing development in AgustaWestland of an advanced physics-based numerical tool able to analyze rotorcraft operations in brownout conditions is presented together with several examples of its application. By means of such computational chain, AgustaWestland is investigating enhanced rotorcraft aerodynamic solutions that may be retrofitted to present aircrafts and incorporated in future designs in order to seriously mitigate brownout. With the aim to contribute to a further extension on brownout knowledge, different rotorcraft configurations were analyzed in the course of this work taking into account different flight conditions in ground effect.

In the early stage of this paper, the AgustaWestland 'Brownout-Simulation-Tool' was presented. This is composed by four different elements, that are: FLIGHTLAB, TOP (Trajectory Optimization Program), ADPANEL-RAS (Rotorcraft Aerodynamics Solver) and ADPANEL-PTM (Particle Transport Model). Subsequently, the capabilities of a single-rotor configuration (which characteristics are based on Puma HC1-like helicopter) to operate in desert environments were compared to those ones exhibited by a dual-rotor system (tiltrotor – V22-like). Numerical results, both in hover and in forward flight at low speeds, confirmed the anecdotal evidence coming from theatre that single-rotor helicopters have got better behaviors with respect to dual-rotor systems [tiltrotors] when operating in brownout conditions. In the final stages of this paper, numerical simulations on the AgustaWestland AW101 helicopter were presented, and its capability to operate in brownout analyzed. Results showed in this work demonstrated the capability of present computational tool to catch the well-known experimental evidence of the enhanced capabilities of present helicopter to mitigate brownout with respect to its competitors.

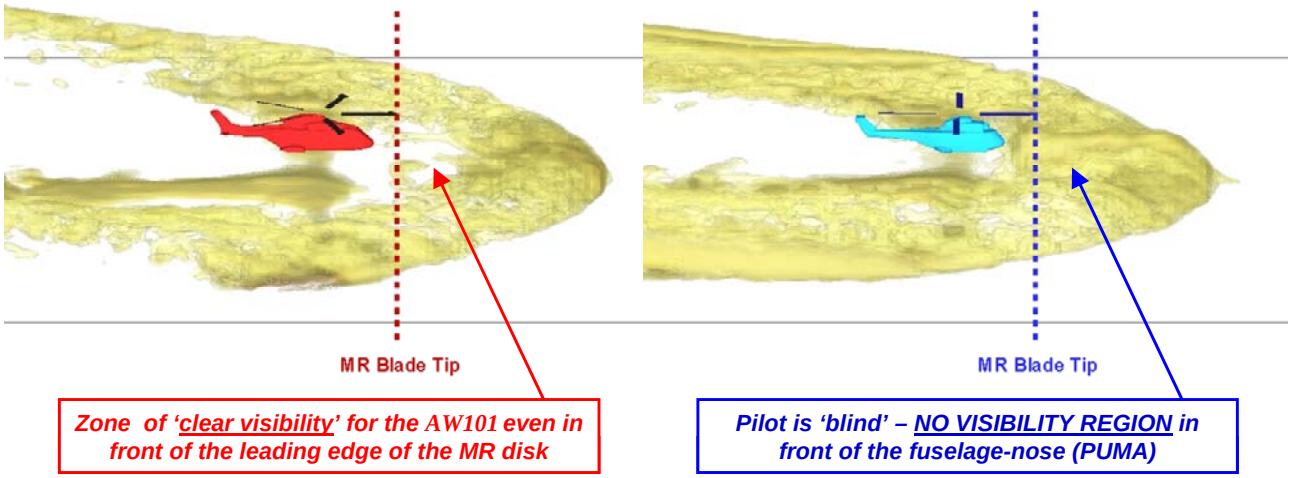

Figure 18 Numerically computed sand-cloud extension and geometry around the AW101 (left) and the PUMA-like (right) in slow-speed forward flight @ 10 Kts [h/R = 1.0]

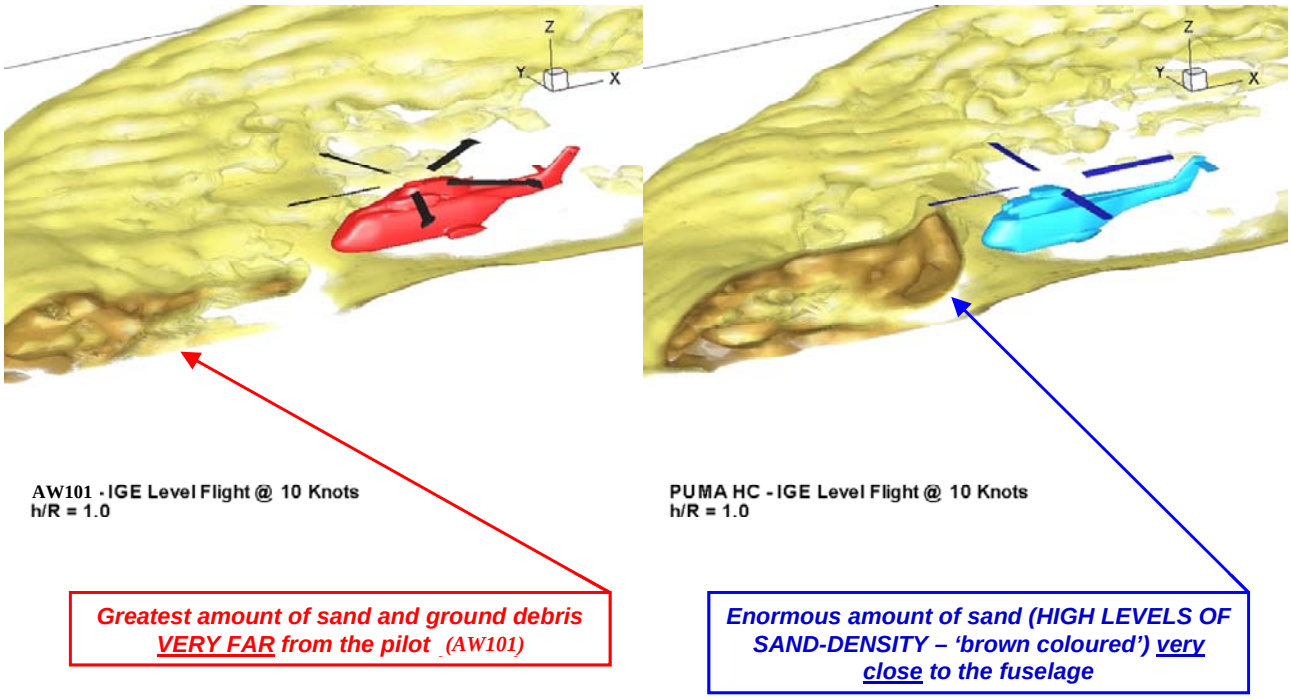

Figure 19 Numerically computed sand-cloud extension, geometry and compactness around the AW101 (left) and the PUMA-like (right) in slow-speed forward flight @ 10 Kts [h/R = 1.0] - ***Zone in brown correspond to high-levels of sand-density***

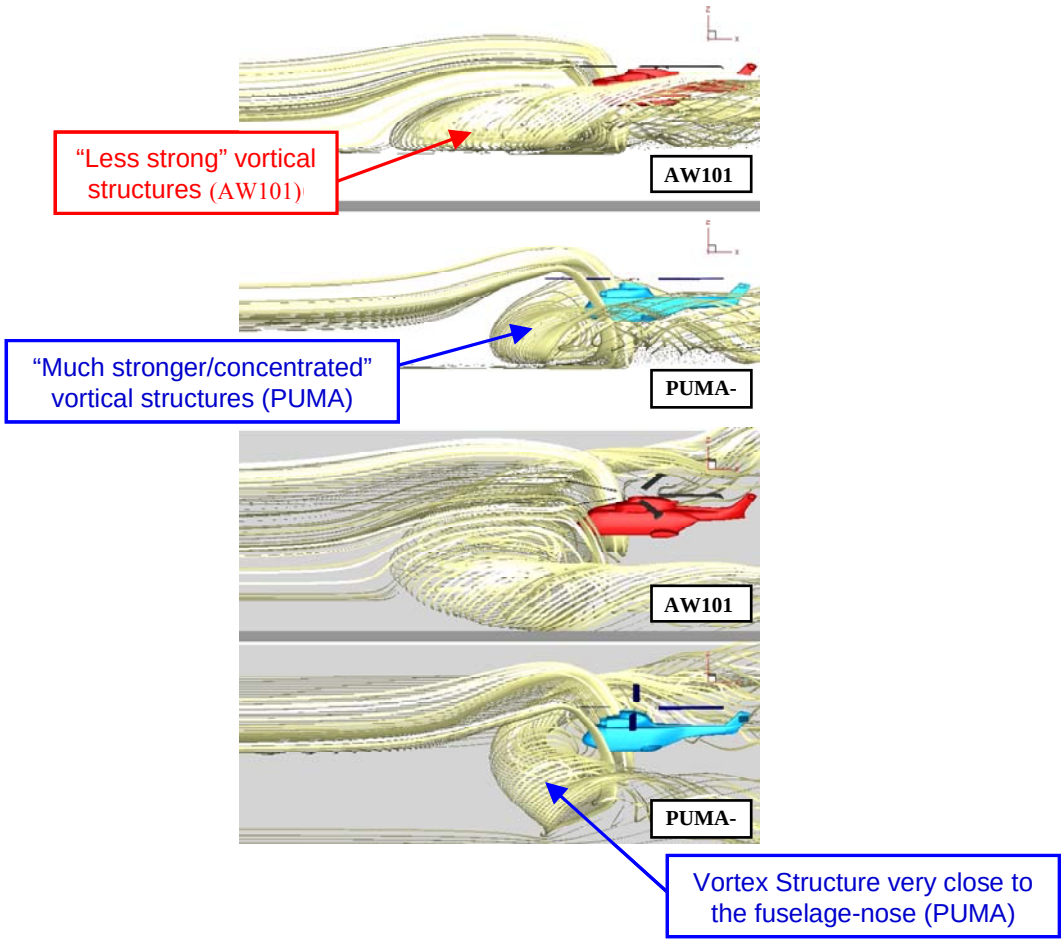

Figure 20 Numerically computed streamlines around the AW101 (top) and the PUMA-like (bottom) for a slow-speed forward flight @ 15 Kts [h/R = 1.0]

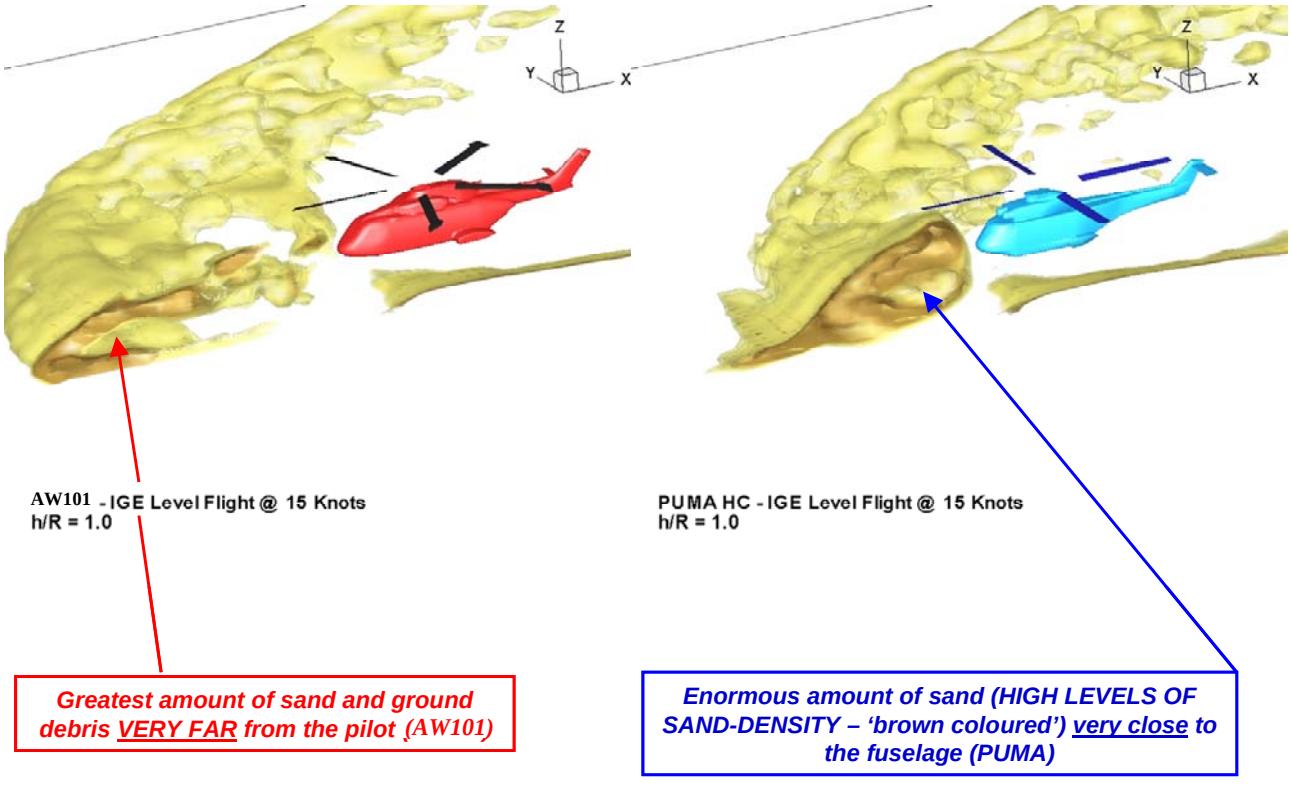

Figure 21 Numerically computed sand-cloud extension, geometry and compactness around the AW101 (left) and the PUMA-like (right) in slow-speed forward flight @ 15 Kts [h/R = 1.0] - *Zone in brown correspond to high-levels of sand-density*

REFERENCES

[1] Brower, M., "Preventing Brownout", Special Operations Technology, Vol. 2, (4), July 2004.

[2] Harrison, R., "EH101 Operations in Brownout Conditions", USAF ADDH2MB Workshop Aerodynamically Designing DoD Helicopters to Mitigate Brownout, University of Maryland, Maryland, December 6-7, 2006.

[3] D'Andrea, A., "Numerical Analysis of Unsteady Vortical flows Generated by a Rotorcraft Operating on Ground: a First Assessment of Helicopter Brownout", 65th American Helicopter Society Annual Forum, Grapevine, TX, May 27-29, 2009.

[4] Phillips, C., Brown, R.E., "The Effect of Helicopter Configuration on the Fluid Dynamics of Brownout", 34th European Rotorcraft Forum, Liverpool, UK, September 16-19, 2008.

[5] Wachspress, D.A., Whitehouse, G.R., Keller, J.D., McClure, K., Gilmore, P., Dorset, M., "Physics Based Modeling of Helicopter Brownout for Piloted Simulation Applications", Interservice/Industry Training, Simulation, and Educational Conference (I/ITSEC), 2008.

[6] Phillips, C., Brown, R.E., "Eulerian Simulation of the Fluid Dynamics of Helicopter Brownout", American Helicopter Society 64th Annual Forum, Montréal, Canada, April 29-May 1, 2008.

[7] Brown, R.E., Line, A.J., "Efficient High-Resolution Wake Modeling Using the Vorticity Transport Equation", AIAA Journal, Vol. 43 (7), July 2005, pp. 1434-1443.

[8] D'Andrea, A., "Unsteady Numerical Simulations of Helicopters and Tiltrotors operating in sandy-desert environments", AHS Specialist's Conference on Aeromechanics, Fisherman's Wharf, San Francisco, California, January 20-22, 2010.

[9] Web-Site: http://www.military-aircraft.org.uk /helicopters/ westland-Puma-like-hc-mk-1.htm

[10] Web Site http: //www.navair.navy.mil/V22-like/

[11] Advanced Rotorcraft Technology, Inc., 1685 Plymouth Street, Suite 250, Mountain View, CA 94043, http://www.flightlab.com.

[12] Bottasso, C.L., Maisano, G., Scorcelletti, F., "Trajectory Optimization Procedures for Rotorcraft Including Pilot Models, with Applications to ADS-33 MTEs, Cat-A and Engine Off Landings", American Helicopter Society 65th Annual Forum, Grapevine, TX, May 27-29, 2009.

[13] D'Andrea, A., "Development of a Multi-Processor Unstructured Panel Code Coupled with a CVC Free Wake Model for Advanced Analyses of Rotorcrafts and Tiltrotors", American Helicopter Society 64th Annual Forum, Montréal, Canada, April 29-May 1, 2008.

[14] D'Andrea, A., Scorcelletti, F., "Enhanced Numerical Simulations of Helicopter Landing Maneuvers in Brownout Conditions", 66th American Helicopter Society Annual Forum, Phoenix, AZ, May 11-13, 2010.

[15] Ramasamy, M., Leishman, J.G., "Reynolds Number Based Blade Tip Vortex Model", American Helicopter Society 61st Annual Forum, Grapevine, TX, June 1-3, 2005.

[16] Bhagwat, M.J., Leishman, J.G., "Generalized Viscous Vortex Model for Applications to Free-Vortex Wake and Aeroacoustic Calculations", American Helicopter Society 68th Annual Forum, Montréal, Canada, June 11-13, 2002.

[17] Marticorena, B., Bergametti, G., "Modeling the Atmospheric Dust Cycle: 1. Design of a soil-derived dust emission scheme", Journal of Geophysical Research, Vol. 100 (D8), August 1995, pp. 16415-16430.

[18] Bagnold, R.A., The Physics of Blown Sand and Desert Dunes, Methuen, London, 1941.

[19] Frazzoli, E., "Robust Hybrid Control for Autonomous Vehicle Motion Planning," Ph.D. Thesis, Massachusetts Institute of Technology, Cambridge, MA, USA, 2001.

[20] Bottasso, C.L., Croce, A., Leonello, D. and Riviello, L., "Rotorcraft Trajectory Optimization with Realizability Considerations," Journal of Aerospace Engineering, Vol. 18, 2005, pp. 146–155.

[21] Griffiths, D.A., Leishman, J.G., "A Study of Dual-Rotor Interference and Ground Effect Using a Free-Vortex Wake Model", American Helicopter Society 58th Annual Forum, Montréal, Canada, June 11-13, 2002.